RSC Advances

PAPER

View Article Online
View Journal | View Issue

Cite this: *RSC Adv.*, 2017, **7**, 11803

The effect of oil type on network formation by protein aggregates into oleogels

Auke de Vries,[ab] Yuly Lopez Gomez,[b] Erik van der Linden[b] and Elke Scholten*[ab]

The aim of this study was to assess the effect of oil type on the network formation of heat-set protein aggregates in liquid oil. The gelling properties of such aggregates to structure oil into so-called 'oleogels' are related to both the particle–particle and particle–solvent interactions. To change these interactions, four different oils (medium chain triglyceride oil, sunflower oil, extra virgin olive oil and castor oil) differing in polarity were used. The rheological properties of the protein aggregate oleogels were determined and compared to gels prepared with hydrophilic and hydrophobic colloidal silica particles at the same concentration. The results show that gel strength of the network formed by protein aggregates is affected by the polarity of the oil, resulting in weaker gels in more polar oils as a result of larger particle–solvent interactions. Similar results were obtained for hydrophilic silica particles. In the case of castor oil, the increased particle–solvent interactions though hydrogen bonds limited gel formation for all particle types. Large deformation rheology shows that protein oleogels exhibit a yielding behaviour under large deformation, but regenerate its elasticity quickly after deformation is reduced. The rapid recovery of the protein network and the fact that the interactions between the protein aggregates can be tuned by changing the characteristics of the oil, may be interesting features for various applications in foods.

Received 10th January 2017
Accepted 7th February 2017

DOI: 10.1039/c7ra00396j

rsc.li/rsc-advances

1. Introduction

In foods, the phenomenon of gelation is governed by a network formation of specific 'building blocks'. In aqueous phases, many biopolymers such as proteins and polysaccharides are able to associate into networks, and provide ample opportunities to create desired textures by varying or combining gelling agents, changing solvent conditions, processing conditions, *etc.*[1] In oil phases, traditionally, structure formation is less diverse and relies on the crystallization of saturated and *trans* fatty acids in triglycerides into a space-spanning network, entrapping the liquid oil. Varying the crystallization rate, shearing conditions, and the composition or amount of saturated fatty acids provide ways to alter the network formation and the physico-chemical properties of the resulting solid-like fat.[2] Although such fatty acids are very useful in food products as they provide oxidative stability, hardness, and plastic deformation, they are also debated because of a possible negative impact on human health by changing the blood cholesterol profile.[3] Although research concerning these health implications of the various fatty acids is still on-going,[4] legislative action has been taken to ban partially hydrogenated oils in food products. Additionally, with regard to the cholesterol composition in the blood, it has been shown that replacement of saturated fats with poly unsaturated fatty acids, as ubiquitously present in liquid oil, has clear health benefits.[5,6] The use of unsaturated fats is therefore highly promoted. The replacement of saturated fats by unsaturated oils, however, is not straightforward as liquid oil can negatively affect the texture of food products.[7,8]

One approach to replace saturated or *trans* fatty acids, which has gained much attention over the last few years, is to use other structuring agents to provide a solid character to liquid oil by the formation of so-called 'oleogels'.[9–12] In many of these oleogels, gelation is achieved by low molecular weight organogelators (LWOG) such as waxes,[13] lecithin,[14,15] phytosterols[16] or monoglycerides.[17] Besides LWOG's, the cellulose derivative ethylcellulose (EC) is studied for its gelling properties in liquid oil. Being hydrophobically modified, this polymer is dispersible in liquid oil at high temperature and forms gels upon cooling.[18]

In the formation of oleogels, the nature of the gelling agent and the nature of the solvent can greatly affect the rheological behaviour. For example, oleogels formed by self-assembly of γ-oryzanol and β-sitosterol into tubules have been shown to be affected by the polarity of the oil.[19] Other researchers, using the same gelators, concluded that next to polarity, also the viscosity of the oil phase affected the self-assembly of the structuring molecules and therefore affected gelation time and the final gel strength.[20] Also in monoglyceride-based oleogels, oils with

[a]*Top Institute Food and Nutrition, Nieuwe Kanaal 9A, 6709 PA Wageningen, The Netherlands*

[b]*Laboratory of Physics and Physical Chemistry of Foods, Wageningen University, P.O. Box 17, 6700 AA Wageningen, The Netherlands. E-mail: elke.scholten@wur.nl*

different polarity and viscosity have shown to affect crystallization and gelation behaviour.[21] Additionally, the fatty acid chain length in the oil affected the rheological behaviour based on a difference in special orientation of the fat crystals.[22] In general, gel strength is decreased when the interactions between the gelator molecules and the oil are enhanced. The interactions depend largely on the chemical composition and the polarity of the oil. In ricinelaidic acid based oleogels, a decrease in the gelation efficiency was observed when the molecules were able to form hydrogen bonding with moieties on different oils.[23] Alternatively, in EC oleogels, an increase in oil polarity or polar compounds increased gel hardness.[24] This effect was related to the better solubility of the EC polymers during heating.

In our previous work, we showed how heat-set whey protein aggregates can be used as effective building blocks for oil gelation.[25] Efficient network formation was achieved by sufficient interactions of hydrophilic nature between the submicron protein aggregates in hydrophobic oil. In general, network formation of such colloidal particles is affected by both particle–particle and particle–solvent interactions. Therefore, a change in solvent type can be used to alter the network formation and the resulting rheological properties. To assess the effect of different solvent conditions, we varied the oil type and investigated the rheological properties of the resulting protein oleogels. For comparison with other colloidal systems, we also examined the rheological behaviour of gels prepared with colloidal silica particles of known surface chemistry, either of hydrophilic or hydrophobic nature.

2. Materials and methods

Materials

Whey protein isolate (WPI, BiPro) was obtained from Davisco Foods International (Le Sueur, MN, USA) with a protein concentration of 93.2% (N × 6.38) and was used as received. Acetone (AR grade) was supplied by Actu-All Chemicals (Oss, The Netherlands). Two types of silica particles were used in this study, a hydrophilic and a hydrophobic fumed silica. Fumed silica, prepared by flame hydrolysis, consists of small, nanometer-sized primary particles that form branched and stable aggregates. Hydrophilic fumed silica (A200) was obtained from Sigma Aldrich and its surface chemistry consists of a high degree of hydroxyl groups. According to the supplier specification, the particles consist of agglomerated, highly branched aggregates of ~0.2–0.3 μm. Hydrophobic silica (R972) was obtained from Evonik Industries (Essen, Germany), for which about 70% of the hydroxyl groups on the surface of the particles were modified by attachment of methyl groups.[26] Both silica particles consisted of agglomerates of small primary particles (Fig. 1) with a specific surface area of 200 $m^2 g^{-1}$ and 130 $m^2 g^{-1}$ for the hydrophilic and hydrophobic silica particles, respectively. For convenience, hydrophobic silica will be referred to as R972 and hydrophilic silica as A200. Four different oils were used in the current study. Extra virgin olive oil (EVO) and sunflower oil were purchased at a local supermarket and used without purification. Medium chain triglyceride oil (MCT) was obtained from Cremer Oleo GmbH (Hamburg, Germany). This highly refined oil consisted predominantly of C8 and C10 fatty acids. Castor oil was obtained from Sigma Aldrich.

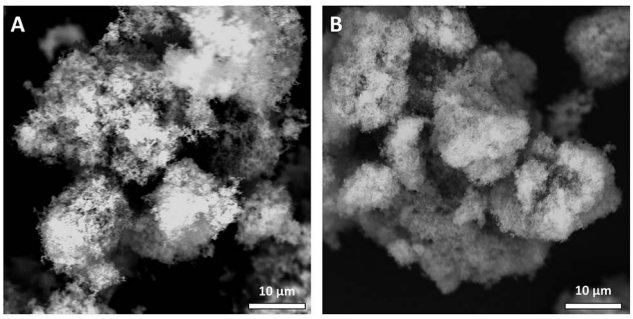

Fig. 1 Scanning electron microscopy (SEM) image of silica particles, (A) hydrophobic R972 silica, (B) hydrophilic A200 silica.

Methods

Oil properties

Viscosity. The viscosity of the oils was determined using a stress-controlled rheometer (AP502, Anton Paar GmbH, Graz, Austria) with a double gap geometry (DG26.7, internal diameter: 24.7 mm, external diameter 26.7 mm). After sample loading, the shear rate was increased from 0.1 to 100 s^{-1}. Measurements were performed in duplicate and all oils behaved as Newtonian liquids.

Interfacial tension. The oil–water interfacial tension was determined using an automated drop tensiometer (ADT, Teclis Tracker, ITCONCEPT, Longessaigne, France). A water droplet (milli-Q, Millipore) with a surface area of 50 mm^2 was created in the different oils. The contact angle was measured under static conditions by keeping the surface area constant, and the interfacial tension was calculated using the available software. Measurements were performed at 20 °C (±0.1 °C), which was maintained by a temperature-controlled water bath. The development of the interfacial tension was followed for 1 h, until a stable value was reached.

Preparation of protein aggregates. WPI powder (4% w/w) was dissolved in demineralized water under continuous stirring at room temperature for 2 h. Afterwards, the pH of the stock solution was adjusted to 5.7 using a 1 M HCl solution. To induce aggregate formation, samples were heated at 85 °C for 15 min using a temperature-controlled water bath. After cooling, the resulting protein dispersion was homogenized using a rotor stator homogenizer (Ultra Turrax, T25, IKA Werke, Germany) at 13 000 rpm for 3 min. The protein aggregates were then collected by centrifugation at 4000*g* (Hermle Z383K, Hermle Labortechnik GmbH, Wehingen, Germany) for 20 min at 20 °C. Hereafter, the pellet was re-dispersed and centrifuged twice with demineralized water to remove remaining soluble protein material.

Preparation of protein oleogels and silica oleogels. To prepare the protein oleogels, the WPI aggregates were transferred to the 4 different oil types using a solvent exchange procedure as described previously.[25] In this procedure, the

polarity of the solvent was changed gradually to remove the surrounding water from the WPI aggregates and replace the continuous phase for oil. In short, 15 g of aqueous pellet, containing the WPI aggregates, was re-dispersed in 150 mL acetone, and mixed thoroughly using rotor stator homogenization at 13 000 rpm for 3 min. Afterwards, the sample was centrifuged at 4000*g* for 20 min at 20 °C. Excess acetone was removed by decanting and the pellet, containing the protein aggregates, was collected. The pellet was then re-dispersed, homogenized and centrifuged as described above once more using acetone to assure water removal, and twice using one of the four oils. The obtained pellet of WPI aggregates in oil was diluted in a ratio of 1 : 10 with oil and left overnight under continuous stirring to allow for evaporation of the remaining acetone. The next day, the protein aggregates were collected by centrifugation at 4000*g* for 20 min at 20 °C. The protein concentration was determined by Dumas (Dumas Flash EA 1112 Series, N Analyser, Thermo Scientific) using a nitrogen conversion factor of 6.38.

To prepare the protein oleogels, the protein concentration was adjusted to 10% w/w by adding the appropriate amount of oil and mixed thoroughly for 3 minutes using a rotor stator homogenizer (3 min, 13 000 rpm). To prepare the silica suspensions, silica powder was added to the liquid oil and mixed thoroughly using rotor stator homogenization for 3 min at 13 000 rpm (the same conditions as for the protein oleogels) to produce a 10% w/w suspension. Hereafter, all samples were degassed using a vacuum pump to remove entrapped air. All values for protein or silica concentration in this paper are given in % w/w.

Rheology

To analyze gel formation, oscillatory rheology experiments were performed using a stress-controlled rheometer (AP502, Anton Paar, GmbH, Graz, Austria). All measurements were performed at 20 °C using a parallel plate ($\varnothing$ = 49.978 mm) setup with sandblasted plates to avoid slip. Before any measurement started, the samples were allowed to equilibrate for 60–120 min at a fixed frequency of 1 Hz and a strain (γ) of 0.01% (which was within the linear viscoelastic region). Frequency sweeps were performed by increasing the frequency logarithmically from 0.01 to 10 Hz at γ = 0.01%. Amplitude sweeps were performed by increasing the strain logarithmically from 0.001 to 100% at a fixed frequency of 1 Hz. To determine the ability of the network to recover, first large deformation was applied at a strain of 100%, and then reduced to 0.01%. The recovery of G' was then monitored for 30 minutes. All measurements were performed in duplicate.

Confocal laser scanning microscopy (CLSM)

The network structure of the protein and silica suspensions was visualized using CLSM. Here, the samples were gently mixed with a drop of rhodamine B solution (0.2%) in ethanol to stain the protein aggregates and silica particles. The resulting network structure was visualized using a Confocal Laser Scanning Microscope (Leica tcs sp5, Leica Microsystems, Wetzlar, Germany).

Scanning electron microscopy (SEM)

To visualize the structure of the silica powders, a Scanning Electron Microscope (Phenom G2 Pro, Phenom-World BV, Eindhoven, and The Netherlands) was used. Using carbon tabs, the powder was fixed onto aluminium stubs (SPI Supplies/Structure Probe Inc., West Chester, USA). The appearance of the powders could be visualized directly without sample pretreatment due to the low voltage used (5 kV).

3. Results and discussion

Appearance and microstructure

In the current study, heat-set whey protein aggregates were used as building blocks for network formation in liquid oil. The protein aggregates were obtained by heating the whey proteins at a pH close to their isoelectric point in aqueous conditions, and the final protein aggregates had a surface averaged diameter ($d_{3,2}$) of 150 nm. These results are in agreement with other papers reporting similar conditions.[27,28] Following their preparation, the protein aggregates were transferred to the oil phase using a solvent exchange procedure, which did not alter their particle size.[25]

At a protein concentration of 10%, self-supporting oleogels had formed, where the liquid oil is entrapped by a network of protein aggregates. The appearance of such a protein oleogel in sunflower oil can be seen in Fig. 2A. To compare the gelling ability of the colloidal protein aggregates with other colloidal particles, two types of fumed silica particles were dispersed in sunflower oil at the same concentration. Hydrophobic R972 silica formed a gel at 10% w/w in sunflower oil, but the network was disrupted when the sample was taken out of the container as the material started to flow (Fig. 2B). In contrast, hydrophilic A200 silica formed a rigid, paste-like structure in sunflower oil at 10% (Fig. 2C). This immediate difference in gelling ability in nonpolar solvents is related to the surface chemistry of the silica particles. The surface of A200 silica consist of hydroxyl groups, whereas for R972 silica, these hydroxyl groups are replaced with methyl groups. In liquid oil, hydrophilic silica is able to from strong particle–particle interactions *via* hydrogen bonds between the hydroxyl groups at the particle surface. Due to the methyl groups on the surface, hydrophobic silica particles have favourable particle–solvent interactions with the surrounding oil and a decreased amount of hydrogen bonds between the particles.[29,30] The microstructure of the network created by the different particles is visualized by CLSM and shown in Fig. 2D–F for the protein aggregates, R972, and A200 respectively. Here, dispersions of 5% were visualized in order to observe the differences in their network structure more clearly. The CLSM image of the protein oleogel (Fig. 2D) shows that the aggregates formed a fractal-like network in the liquid oil, resulting in gel formation. The R972 silica particles, on the other hand, were distributed homogeneously throughout the suspending oil, which can be attributed to the more hydrophobic character of the particles (Fig. 2E). Due to the presence of strong hydrogen bonds between the hydrophilic particles, A200 silica

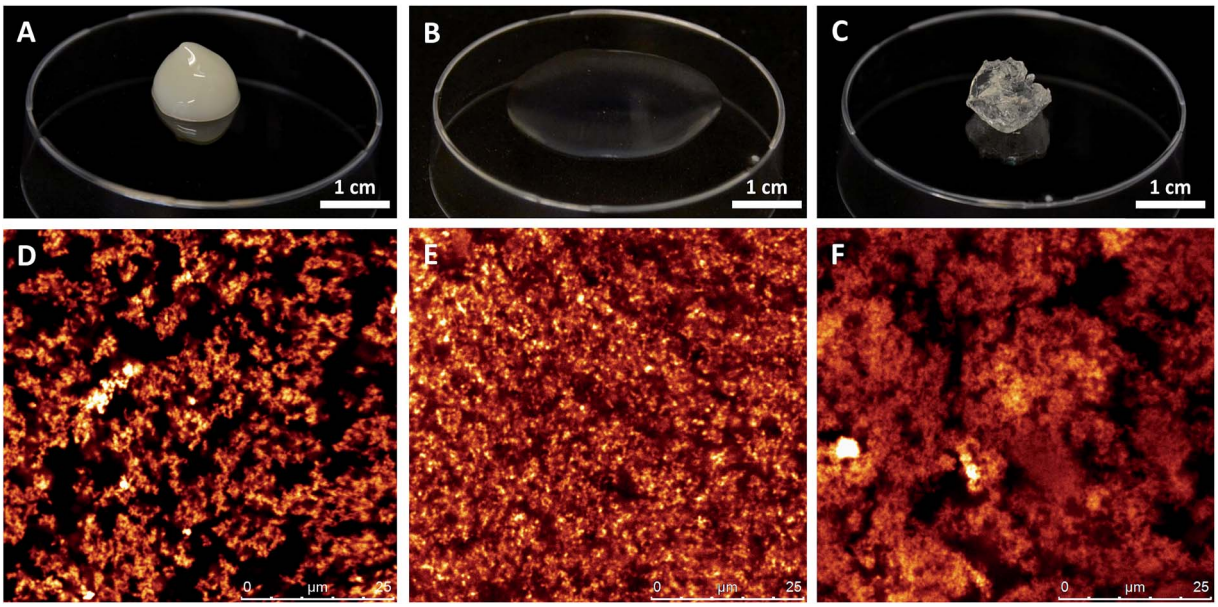

Fig. 2 Appearance of 10% dispersions in sunflower oil of whey protein aggregates (A), hydrophobic silica R972 (B), hydrophilic silica A200 (C) and corresponding CLSM images (D–F). Samples for CLSM were diluted to 5%.

(Fig. 2F) formed a fractal-like network structure. Compared with both silica particles, the protein aggregates seem to form a network consisting of denser clusters. Most likely, the silica particles have a higher porosity and a larger surface area compared to the protein aggregates, which resulted in a finer network. Nevertheless, the tendency for network formation is attributed to the balance between particle–solvent and particle–particle interactions and in this regard, protein aggregates show a higher similarity to the hydrophilic silica particles.

Another interesting feature is that the protein oleogel was opaque, whereas both silica oleogels were transparent. This difference in appearance can be explained by taking the refractive indices (RI) of the materials into account. Silica particles have a RI of ~1.47, which is close to that of sunflower oil (~1.46–1.47). For protein solutions, the RI depends on the concentration, and for largely dehydrated proteins, the RI is ~1.54.[31]

Solvent characteristics

Network formation by colloidal particles suspended in a solvent is largely dependent on the surface chemistry of the particles and the nature of the solvent. Therefore, four different oil types were chosen to prepare the oleogels; medium chain glyceride oil (MCT), extra virgin olive oil (EVO), sunflower oil, and castor oil. Characteristics of these oils can be found in Table 1. MCT oil consists mainly of medium chain (C:8 and C:10) saturated fatty acids, is highly refined and has a relative low viscosity. Sunflower oil and EVO both mainly consist of oleic (C18:1) and linoleic (C18:2) acid, where EVO can also contain up to 20% palmitic acid (C16:0).[32] The main difference between sunflower oil and EVO is the degree of refinement. Sunflower oil is a refined oil with minor polar components, with the exception of tocopherols. EVO on the other hand is a cold pressed, unrefined oil which can contain a substantial amount (up to 2%) of polar molecules such as polyphenols, phosphatides, pigments, and sterols.[32] Given the different composition, we propose that this has an influence on the polarity of the different oils. Here, we use the oil–water interfacial tension as a measure for oil polarity. Due to the high level of refinement of the MCT oil, the polarity of this oil is the lowest, which is evidenced by the highest oil–water interfacial tension among the used oils in this study (Table 1). Both sunflower oil and EVO are less pure, and therefore have a slightly higher polarity. As seen by the difference in interfacial tension, EVO had a lower interfacial tension than sunflower oil, as expected by the larger amount of minor components present. Castor oil consists mainly of ricinoleic acid, a C18:1 carbon fatty acid with a hydroxyl group at the C12 position. As a result of these hydroxyl groups, this oil is more polar than the other oils studied, as seen by the lowest value for the interfacial tension. The viscosities of the oils differ significantly, where MCT has the lowest viscosity and castor oil is the most viscous oil as shown in Table 1. Based on the interfacial tension, the polarity of the oils studied range from low to high polarity as MCT < sunflower oil < EVO < castor oil.

Table 1 Viscosity and oil–water interfacial tension of the oils used to form oleogels

Oil type	Viscosity at 20 °C [mPa s]	Oil–water interfacial tension at 20 °C [mN m^{-1}]
MCT oil	29.8 (±0.1)	26.5 (±0.4)
Sunflower oil	63.3 (±0.1)	24.4 (±0.1)
EVO	80.1 (±0.1)	14.7 (±0.1)
Castor oil	1045.0 (±5.0)	11.7 (±0.1)

Small amplitude oscillatory rheology

Using these oils, protein aggregates were dispersed at a concentration of 10% to create oleogels and we examined their rheological behaviour. First, we focus on the protein oleogels prepared in MCT, EVO and sunflower oil, since castor oil had a large impact on the rheological behaviour due to its different chemical composition, as will be discussed in detail below. The storage modulus, G', and the loss modulus, G'', as a function of the frequency are shown in Fig. 3. Since G' is larger than G'' in all cases and G' is largely independent of the applied frequency, this indicates that all systems can be classified as gels. To determine the effect of changing the particle surface chemistry on network formation, the two types of silica particles with known surface chemistry were used for comparison. Regardless of the type of oil used, G' was found to be much higher for the hydrophilic A200 silica than the hydrophobic R972 silica. A200 silica samples were independent on the applied frequency, whereas for R972 silica, this dependency was distinctly higher. For R972 silica, a cross-over between G' and G'' at high frequencies can be seen, indicating weaker gel network formation than in the case A200 silica particles were used. Due to the methyl groups on the surface of the particles, R972 silica has increased favourable interactions with the surrounding nonpolar solvents and a lower ability for particle–particle hydrogen bonds. In contrast, A200 silica has less favourable interactions with the surrounding solvent, and an increased ability for particle–particle interactions through hydrogen bonds. This is in accordance with other reports on the gelling behaviour of these two types of silica particles.[29,33]

Protein aggregates at the same concentration formed gels with a gel strength in between that of the two types of silica particles, both in magnitude of G' as well as in the frequency dependency of G'. Since protein aggregates are amphiphilic, the ability for network formation in oil compared to the hydrophilic A200 silica is lower, due to fewer particle–particle interactions, but higher compared to the hydrophobic R972 silica. Another reason for the lower gel strength of the protein aggregates compared to A200 silica could be the difference in density of the network. Looking at the CLSM images (Fig. 2), the protein aggregates formed a coarser, more open network compared to the more finely dispersed A200 silica. Colloidal silica consist of highly porous particles with a high surface area, which could lead to more particle–particle interactions compared to the protein aggregates and hence higher gel strength.

Besides the surface chemistry of the particles, also the nature of the solvent has an effect on the ability to form colloidal networks. For better comparison, values for G' and the loss tangent (tan δ, G''/G' *i.e.* the solid-like character of the gel) for the different gel systems is summarized in Fig. 4. For A200 silica, using a polar EVO decreased G' and increased tan δ, indicating a weaker network formation compared to gels made with the apolar MCT oil. Interestingly, for R972 silica this effect is reversed, *i.e.* G' increased and tan δ decreased with increasing polarity. Notice that the change in polarity has a larger effect on the hydrophobic then the hydrophilic particles. G' decreases roughly a factor 2 for A200 silica, whereas for R972 silica at the same concentration, G' increased roughly with a factor 13. The decrease in gel strength for the hydrophilic A200 silica particles can be explained by the increase in particle–solvent interactions as a function of increased polarity changing from MCT to EVO. Similarly, an increase in gel strength for hydrophobic R972 particles is obtained as a function for increasing polarity, as the more apolar MCT oil favours more particle–solvent interactions than the more polar EVO.

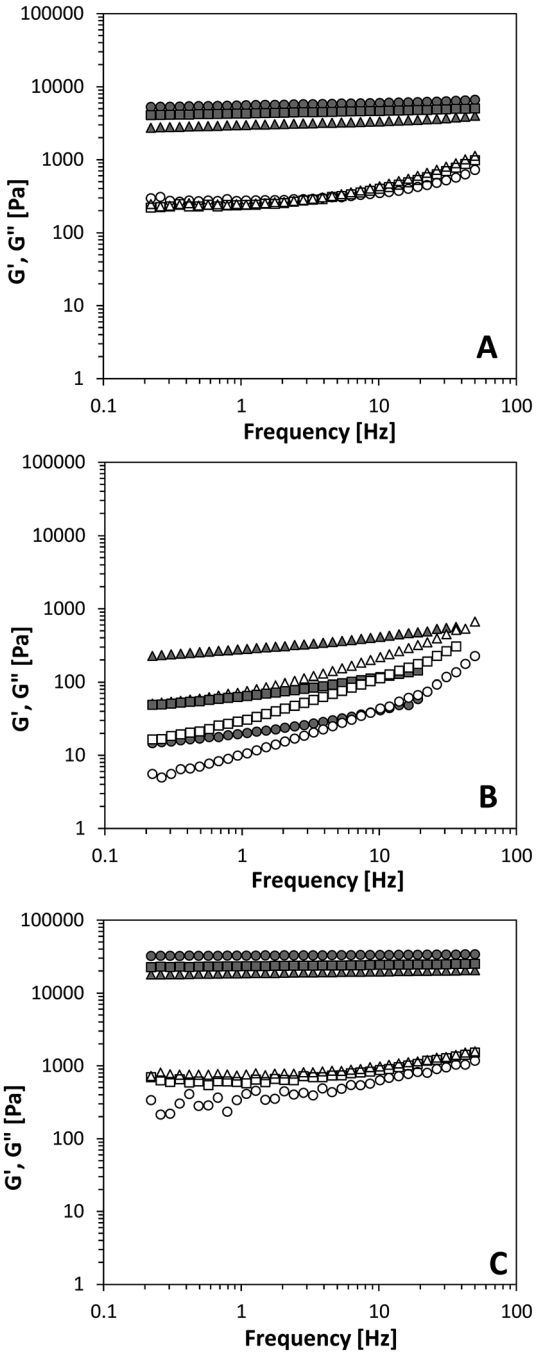

Fig. 3 Frequency sweeps of 10% protein aggregates (A), hydrophobic R972 silica (B), and hydrophilic A200 silica (C) in MCT oil (○), sunflower oil (□) and olive oil (△). Filled symbols: G', open symbols: G''.

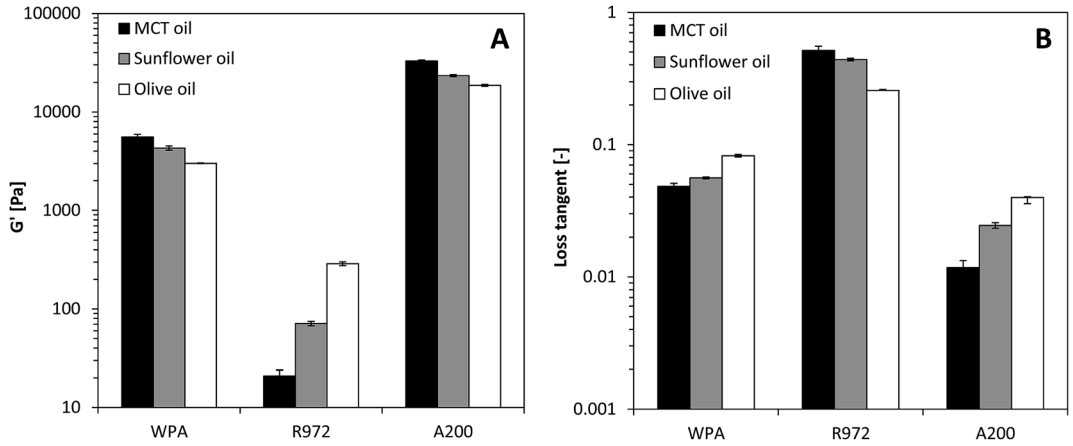

Fig. 4 G' (A) and loss tangent (B) of 10% whey protein aggregates (WPA), hydrophobic silica (R972) and hydrophilic silica (A200) in different oils.

Using different oil types for structure formation by the protein aggregates, G' increased and tan δ decreased as EVO < sunflower oil < MCT oil, indicating a higher amount of protein–solvent interactions in a more polar environment, giving weaker gel strength. Similar to A200 silica, G' decreased roughly two-fold as the polarity of the oil type increases. The results indicate that the strength of the network formed by protein aggregates is affected by the polarity of the solvent, resulting in weaker gels in more polar oils.

The most polar oil used in this study was castor oil, as shown by the lowest oil–water interfacial tension. This high polarity is caused by ricinoleic acid, which has a hydroxyl group at the C12 position. When attempting to create oleogels in castor oil using the protein aggregates, we were not able to acquire a dispersion of sufficient concentration, and therefore the rheological behaviour could not be determined. For both silica particles, as shown in Fig. 5A, no gel formation was observed as $G'' > G'$ for most of the frequencies studied and G'' was almost proportional to the applied frequency. Hydrophilic A200 silica showed a cross-over between G' and G'' at low frequency, but G'' was larger than G' for the entire frequency range for the hydrophobic R972 silica. This indicates that no network formation was achieved by either of the silica particles. As shown in the CLSM micrographs in Fig. 5B and C, both silica particles were dispersed evenly throughout the castor oil, indicating few particle–particle interactions and poor network formation. Based on the increased polarity, we would indeed expect a decrease in gel strength for the hydrophilic silica. As shown by Raghavan and co-workers,[30] the main driving force for network formation between silica particles is the formation of particle–particle interactions through hydrogen bonds. Instead of strong particle–particle interactions, the high content of hydroxyl groups in castor oil favoured particle–solvent interactions, causing a 'solvation layer' around the particles and therefore inhibited gel formation. For the hydrophobic silica, on the other hand, we would expect an increase in gel strength based on the results discussed previously. In the case of castor oil, hydrogen bonds can also occur between the predominantly hydrophobic particles and the solvent, even if the high polarity of the solvent would favour less particle–solvent interactions. For all types of particles, this increased particle–solvent hydrogen bonds prevented gel formation. The network formation can therefore not only be controlled by the polarity, but also by the presence of specific chemical groups on the solvent molecules.

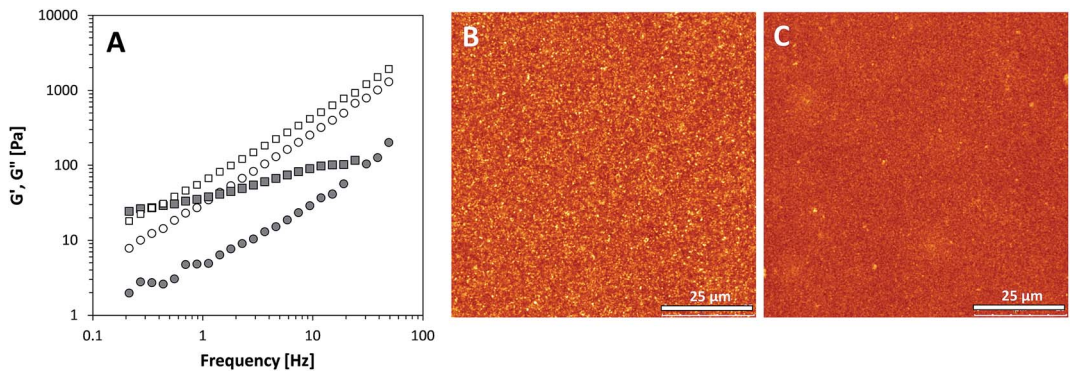

Fig. 5 Frequency sweep (A) of 10% hydrophilic A200 silica (□) and hydrophobic R972 silica (○) in castor oil. CLSM image (B) of 5% R972 and (C) 5% A200 in castor oil. Filled symbols: G', open symbols: G''.

Large deformation and structure recovery

Besides the formation of elastic networks, depending on the interactions between the colloidal particles to build a structure, properties like resistance against structure breakdown and structure recovery are important aspects for different applications. Therefore, we examined the structure breakdown of the different particles using large deformation rheology. Fig. 6 shows the rheological behaviour of the oleogels as a function of the applied strain, where the linear viscoelastic regime (LVR) is defined as the strain value where G' is independent on the applied strain until a certain critical value (γ_c).

As shown in Fig. 6B and C, A200 silica oleogels show a somewhat longer LVR compared to R972 silica, indicating the network is less prone to yielding. Most likely, this can be attributed to the higher surface area of the A200 silica and the increased ability to form particle–particle interactions through hydrogen bonds in nonpolar media, giving rise to a more rigid network. Compared to both silica particles, the gels prepared with protein aggregates had a distinct lower γ_c. Based solely on their amphiphilic nature, we would expect that structure breakdown by yielding would be an intermediate between the hydrophilic and hydrophobic particles. The results show that the amphiphilicity of the protein aggregates is not the only parameter to determine the yielding behaviour of the network. Looking again at the microstructure of the gels in Fig. 2, the more densely packed network by the protein aggregates compared to the silica particles could explain this different behaviour, as the larger mesh sizes and the lower amount of connections between larger flocs in the colloidal network would be more prone to yielding phenomena. Similar effects were observed for Ca^{2+}-induced WPI gels, where coarser networks were formed for increasing Ca^{2+} concentration, which resulted in gels with a lower fracture strain.[34]

As shown in Fig. 6, γ_c was not substantially affected by the oil type, indicating that indeed the network structure is more dominant for yielding phenomena. An exception is seen in the case for EVO, where a lower γ_c is observed for both the A200 silica and the protein aggregates. As EVO is not a very pure oil, the structure breakdown might be related to the presence of polar components having a high affinity for the particle surface, leading to fewer or less strong interactions. An interesting feature is observed for strain amplitudes around γ_c. For the gels made with A200 silica and protein aggregates, G'' shows a weak strain overshoot in the region of γ_c, which is not detected in the R972 gels. This overshoot for G'' is characteristic for many flocculated gel structures.[35,36] Deformation of a network, as is done in these experiments, is a process where two phenomena, structure loss and structure creation, simultaneously occur due to breakage and reformation of network junctions. The type of behaviour observed when increasing the strain amplitude depends on which of these two phenomena is dominant. Although difficult to quantify the magnitude of these processes, the change in the moduli can provide qualitative information as described in a paper by Hyun and co-workers,[37] where the authors define a loss rate parameter and a creation rate parameter. Strain thinning behaviour, or 'type I' behaviour, is observed when the loss parameter is positive and the creation parameter is negative, giving rise to a decrease in both moduli. In this case, the structural elements align with the applied flow field and lose network junctions that do not reform during deformation, as we observe for the hydrophobic R972 samples. In 'type III' behaviour, both parameters are positive, but the creation parameter is smaller than the loss parameter, giving rise to a weak strain overshoot for G'' as we observe for both the protein aggregate gels and the A200 gels. As the two types of

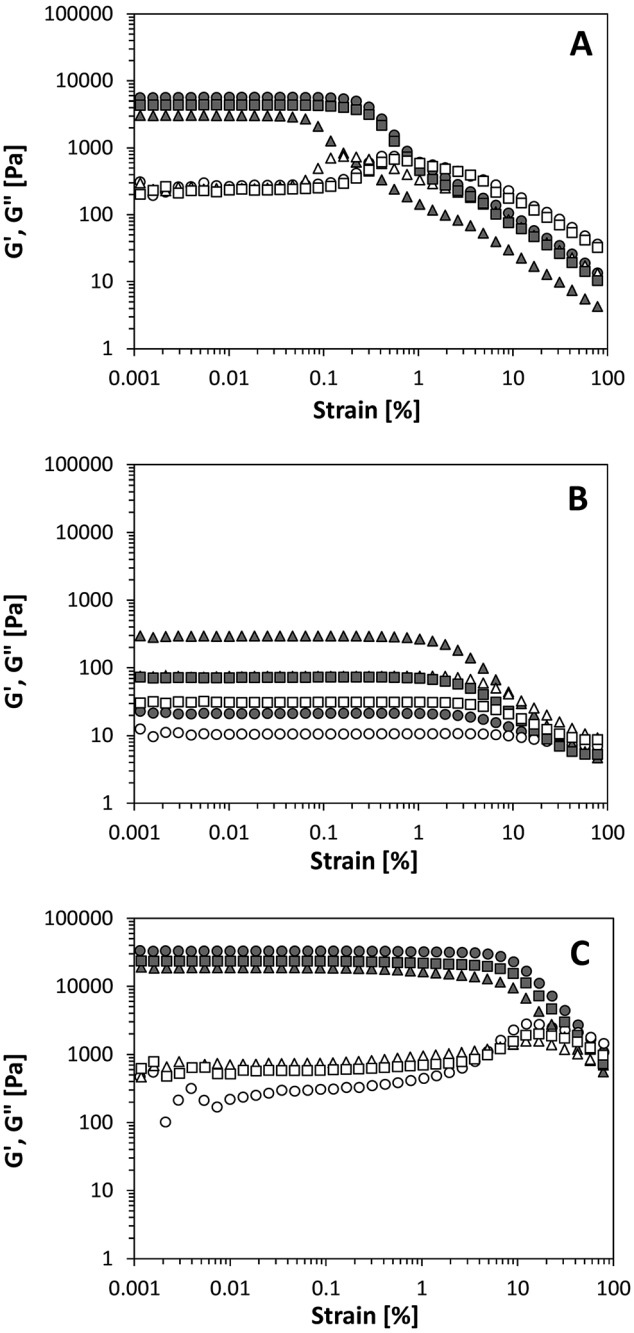

Fig. 6 Large deformation properties of 10% WPA oleogels (A), hydrophobic R972 silica oleogels (B) hydrophilic A200 silica oleogels (C), in MCT oil (○), sunflower oil (□) and olive oil (△). Filled symbols: G', open symbols: G''.

silica show a different behaviour during deformation, this indicates that the rate of structure loss and structure formation is dependent on the surface chemistry of the particles and the strength of the particle–particle interactions. Since a weak strain overshoot is observed for the more hydrophilic particles, rapid structure formation is most likely due to the rate of hydrogen bond formation between the particles. To further assess the ability of the network to restore after deformation is applied, we examined the structure reformation over time at low deformation after the network was subjected to high strains.

Structure recovery

After subjecting the different gels to large deformation (γ = 100%) to induce structure breakdown, the strain was reduced to $\gamma = 0.01\%$ (which was within the linear viscoelastic regime) to examine the structure recovery, or thixotropic behaviour, over time. During structure breakdown, network junctions between interacting colloidal particles or fractal flocs of these particles are broken due to the applied large deformations. Under subsequent non-destructive low deformations, these junctions are then reformed, restoring the network. The recovery of G' was followed for 30 minutes and the results can be found in Fig. 7A–C. As shown, the development of G' over time showed a power law dependence over time for all samples following $G' \sim t^n$. In all samples, it was found that $n < 1$ (Table 2), which indicates a self-delaying process where the rate of change, dG'/dt, decreases over time. This power law dependency was also observed for other systems, such as clay dispersions[38] and fat crystals.[39] Important to note is that during recovery, gels were reformed for which $G' > G''$ in all samples.

Fig. 7A shows a rapid structure recovery for the protein aggregates, where most of the recovery occurred in the first minute after reduction of the strain amplitude. In literature, a rapid structure recovery was also observed for silica particles and nano-diamond particles in mineral oil[40,41] or fat crystal networks.[39] Similar to the case of protein aggregates, the structure recovery of the A200 silica network was fast and can be described by a power law exponent n close to zero (Table 2). Therefore, most of the disrupted network, as a result of detachment of the particles or clusters of particles from the network by

Table 2 Exponent n for structure recovery after deformation, determined by the best fit of $G' \sim t^n$

	Structure recovery exponent n particle type		
Oil type	WPA	R972	A200
MCT	0.09 (±0.00)	0.44 (±0.05)	0.05 (±0.01)
Sunflower	0.09 (±0.00)	0.56 (±0.01)	0.04 (±0.00)
EVO	0.14 (±0.00)	0.72 (±0.01)	0.05 (±0.00)

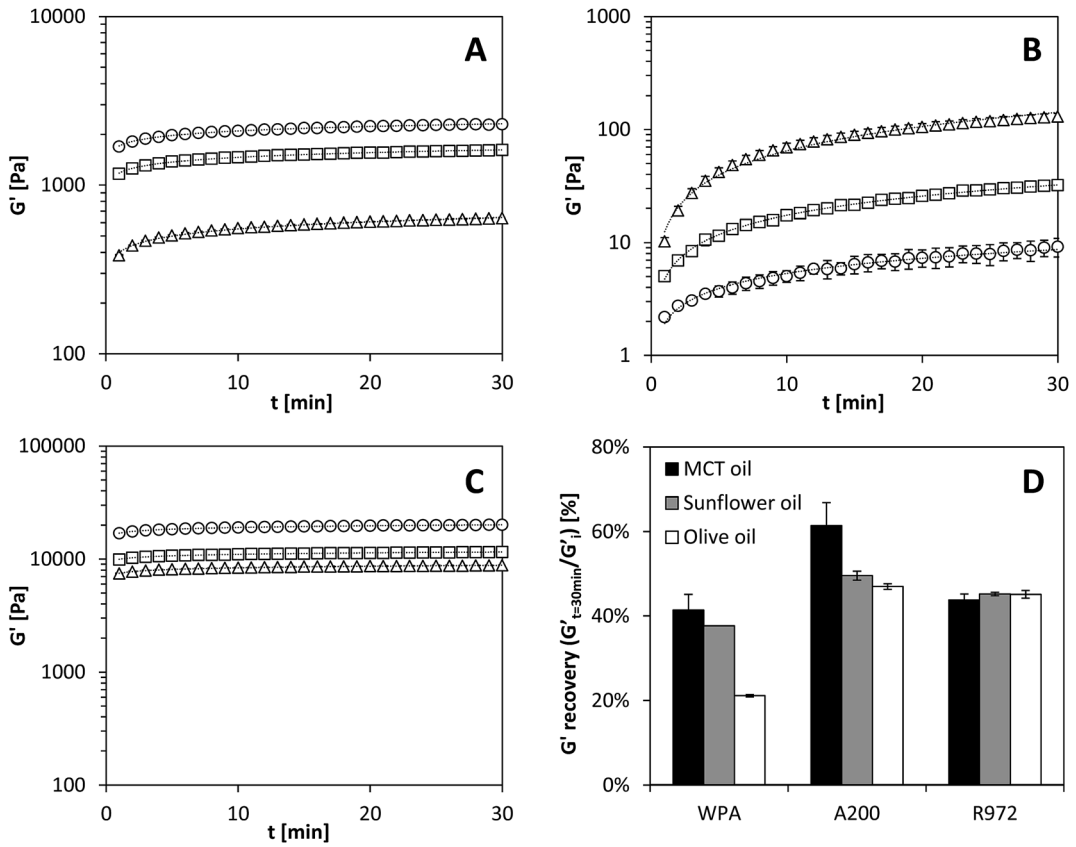

Fig. 7 Structure recovery after deformation at 100% strain over time for oleogels prepared with 10% whey protein aggregates WPA (A), hydrophobic R972 silica (B), hydrophilic A200 silica (C) in MCT oil (○), sunflower oil (□) and olive oil (△). The solid lines represent the best fit to $G' \sim t^n$. (D) summarizes the obtained values for G' recovery after 30 minutes as %.

applying high strains, almost instantaneously reformed by creating new junctions. For the hydrophobic R972 silica particles, however, the network recovery was slower (Fig. 7B) compared to that of the hydrophilic A200 silica or protein aggregates. These results can most likely be related to the affinity of the particles for the solvent. In the case of the hydrophilic silica particles and the protein aggregates, the low affinity for the solvent leads to particle–particle interactions that dominate over particle–solvent interactions in oil. The strong particle–particle interactions gave rise to a rapid G' recovery for both A200 silica and protein aggregates upon lowering the strain.

Using a different oil type did not result in an observable difference for the structure recovery rate for A200 silica and for the protein oleogels. Since the recovery is almost instantaneous, it is likely that the differences could not be seen with the current experimental setup. In contrast, the characteristics of the different oils did have an effect on the recovery rate for gels made with R972 silica. In these gels, the recovery rate over time (dG'/dt) was lower for apolar MCT oil than for the polar EVO. This effect is most likely related to more favourable particle–particle interactions in the polar EVO, compared to more particle–solvent interactions in the apolar MCT oil.

Fig. 7D shows the amount of G' recovery for different oil types after 30 minutes, which was defined as the G' after 30 minutes recovery time divided over the initial gel strength (G'_i) before large deformation. The network of protein aggregates recovered towards 20–40% of their original G' after 30 minutes, depending on the oil type used. Largest recovery was measured for MCT oil, followed by sunflower oil and EVO. Similar behaviour was measured for A200 silica, where the same effect of oil type on the extend of structure recovery was measured, although the recovery was higher (50–60%). This effect of oil type is consistent with the larger amount of particle–particle interactions observed for a more apolar oil and more hydrophilic particles. The network of the hydrophobic silica particles recovered to about 45% of their original value for G', but their recovery did not depend on oil type within the timeframe of the experiment. The lower G' recovery for the protein aggregates compared to the two types of silica particles may be explained by the denser network structure of the protein aggregates. Upon deformation of such a dense network with larger clusters and a relative large mesh size, less bonds are re-formed between the proteins aggregates compared to the finer network of silica particles. This could be due to the larger surface area of the silica particles and subsequently more contact points between the particles. However, given that protein oleogels are able to flow under large deformation, but regenerate its elastic network quickly after deformation is reduced, this behaviour could provide benefits to a variety of food applications.

4. Conclusions

Whey protein based oleogels (10% protein) were prepared using heat-set whey protein aggregates. Since the particle–particle interactions between the aggregates in oil can be affected by oil composition, we prepared protein oleogels in different oil types; Medium Chain Triglyceride (MCT) oil, sunflower oil, extra virgin olive oil (EVO) and castor oil. The oils varied in polarity and chemical composition. For comparison, we used two types of silica particles of known surface chemistry, *i.e.* hydrophilic and hydrophobic silica, to prepare silica oleogels at the same concentration. All particles were able to provide structure to MCT oil, sunflower oil and EVO, where $G' > G''$. The change in oil type resulted in a difference in particle–particle and particle–solvent interactions, which in turn affected the rheological behaviour. For protein aggregates, an increase in oil polarity resulted in a decrease in G' due to more favourable particle–solvent interactions. In castor oil, we were unable to create gels with either silica particles or protein aggregates. This effect can be attributed to the ability of the oil to form hydrogen bonds with the particles, preventing particle–particle interactions. Large deformation behaviour of protein oleogels showed structure breakdown and yielding behaviour of the gels followed by rapid recovery of the network after deformation was reduced. Rapid recovery after deformation and the fact that the interactions between the protein aggregates in oil can be tuned by changing the characteristics of the oil, may be interesting features for various applications in foods.

Acknowledgements

The authors would like to thank Jan Klok (NIZO Food Research, Ede, The Netherlands) for his help with the CLSM experiments. This research was funded by the Top Institute Food and Nutrition.

References

1 S. Banerjee and S. Bhattacharya, Food gels: gelling process and new applications, *Crit. Rev. Food Sci. Nutr.*, 2012, **52**(4), 334–346.
2 A. G. Marangoni, *et al.*, Structure and functionality of edible fats, *Soft Matter*, 2012, **8**(5), 1275–1300.
3 R. P. Mensink and M. B. Katan, Effect of dietary trans fatty acids on high-density and low-density lipoprotein cholesterol levels in healthy subjects, *N. Engl. J. Med.*, 1990, **323**(7), 439–445.
4 R. P. Mensink, *et al.*, The Increasing Use of Interesterified Lipids in the Food Supply and Their Effects on Health Parameters, *Adv. Nutr.*, 2016, **7**(4), 719–729.
5 F. B. Hu and W. C. Willett, Optimal diets for prevention of coronary heart disease, *J. Am. Med. Assoc.*, 2002, **288**(20), 2569–2578.
6 R. P. Mensink, *et al.*, Effects of dietary fatty acids and carbohydrates on the ratio of serum total to HDL cholesterol and on serum lipids and apolipoproteins: A meta-analysis of 60 controlled trials, *Am. J. Clin. Nutr.*, 2003, **77**(5), 1146–1155.
7 C. C. Akoh, Fat replacers, *Food Technol.*, 1998, **52**(3), 47–53.
8 M. L. Sudha, *et al.*, Fat replacement in soft dough biscuits: Its implications on dough rheology and biscuit quality, *J. Food Eng.*, 2007, **80**(3), 922–930.

9 A. Marangoni, Organogels: An Alternative Edible Oil-Structuring Method, *J. Am. Oil Chem. Soc.*, 2012, **89**(5), 749–780.
10 A. R. Patel and K. Dewettinck, Edible oil structuring: an overview and recent updates, *Food Funct.*, 2016, **7**(1), 20–29.
11 M. A. Rogers, Novel structuring strategies for unsaturated fats – Meeting the zero-trans, zero-saturated fat challenge: A review, *Food Res. Int.*, 2009, **42**(7), 747–753.
12 M. A. Rogers, A. J. Wright and A. G. Marangoni, Oil organogels: the fat of the future?, *Soft Matter*, 2009, **5**(8), 1594–1596.
13 A. I. Blake, E. D. Co and A. G. Marangoni, Structure and physical properties of plant wax crystal networks and their relationship to oil binding capacity. JAOCS, *J. Am. Oil Chem. Soc.*, 2014, **91**(6), 885–903.
14 C. V. Nikiforidis and E. Scholten, Self-assemblies of lecithin and α-tocopherol as gelators of lipid material, *RSC Adv.*, 2014, **4**(5), 2466–2473.
15 M. Pernetti, *et al.*, Structuring edible oil with lecithin and sorbitan tri-stearate, *Food Hydrocolloids*, 2007, **21**(5–6), 855–861.
16 A. Bot and W. G. M. Agterof, Structuring of edible oils by mixtures of γ-oryzanol with β-sitosterol or related phytosterols, *J. Am. Oil Chem. Soc.*, 2006, **83**(6), 513–521.
17 S. Da Pieve, *et al.*, Shear Nanostructuring of Monoglyceride Organogels, *Food Biophys.*, 2010, **5**(3), 211–217.
18 M. Davidovich-Pinhas, S. Barbut and A. G. Marangoni, The gelation of oil using ethyl cellulose, *Carbohydr. Polym.*, 2015, **117**, 869–878.
19 H. Sawalha, *et al.*, The influence of the type of oil phase on the self-assembly process of γ-oryzanol + β-sitosterol tubules in organogel systems, *Eur. J. Lipid Sci. Technol.*, 2013, **115**(3), 295–300.
20 S. Calligaris, *et al.*, Effect of Oil Type on Formation, Structure and Thermal Properties of γ-oryzanol and β-sitosterol-Based Organogels, *Food Biophys.*, 2013, **9**(1), 69–75.
21 F. Valoppi, *et al.*, Influence of oil type on formation, structure, thermal and physical properties of monoglyceride-based organogel, *Eur. J. Lipid Sci. Technol.*, 2016, DOI: 10.1002/ejlt.201500549.
22 A. J. Martins, *et al.*, Beeswax organogels: Influence of gelator concentration and oil type in the gelation process, *Food Res. Int.*, 2016, **84**, 170–179.
23 A. J. Wright and A. G. Marangoni, Formation, structure, and rheological properties of ricinelaidic acid-vegetable oil organogels, *J. Am. Oil Chem. Soc.*, 2006, **83**(6), 497–503.
24 A. J. Gravelle, *et al.*, Influence of solvent quality on the mechanical strength of ethylcellulose oleogels, *Carbohydr. Polym.*, 2016, **135**, 169–179.
25 A. de Vries, *et al.*, Protein oleogels from heat-set whey protein aggregates, *J. Colloid Interface Sci.*, 2017, **486**, 75–83.
26 H. Ferch, The use of hydrophobic AEROSIL in the coatings industry, *Technical Bulletin Pigments No. 18*, 1993.
27 C. Schmitt, *et al.*, Influence of protein and mineral composition on the formation of whey protein heat-induced microgels, *Food Hydrocolloids*, 2011, **25**(4), 558–567.
28 C. Schmitt, *et al.*, Internal structure and colloidal behaviour of covalent whey protein microgels obtained by heat treatment, *Soft Matter*, 2010, **6**(19), 4876–4884.
29 A. R. Patel, *et al.*, Fumed silica-based organogels and 'aqueous-organic' bigels, *RSC Adv.*, 2015, **5**(13), 9703–9708.
30 S. R. Raghavan, *et al.*, Colloidal interactions between particles with tethered nonpolar chains dispersed in polar media: Direct correlation between dynamic rheology and interaction parameters, *Langmuir*, 2000, **16**(3), 1066–1077.
31 R. Barer and S. Tkaczyk, Refractive Index of Concentrated Protein Solutions, *Nature*, 1954, **173**(4409), 821–822.
32 P. Inglese, *et al.*, Factors Affecting Extra-Virgin Olive Oil Composition, in *Horticultural Reviews*, 2011, pp. 83–147.
33 S. A. Khan and N. J. Zoeller, Dynamic rheological behavior of flocculated fumed silica suspensions, *J. Rheol.*, 1993, **37**(6), 1225–1235.
34 S. Barbut, Effects of calcium level on the structure of pre-heated whey protein isolate gels, *LWT–Food Sci. Technol.*, 1995, **28**(6), 598–603.
35 M. Kawaguchi, M. Okuno and T. Kato, Rheological properties of carbon black suspensions in a silicone oil, *Langmuir*, 2001, **17**(20), 6041–6044.
36 C. Derec, *et al.*, Aging and nonlinear rheology in suspensions of polyethylene oxide-protected silica particles, *Phys. Rev. E: Stat., Nonlinear, Soft Matter Phys.*, 2003, **67**(6), 061403.
37 K. Hyun, *et al.*, A review of nonlinear oscillatory shear tests: Analysis and application of large amplitude oscillatory shear (LAOS), *Prog. Polym. Sci.*, 2011, **36**(12), 1697–1753.
38 N. Willenbacher, Unusual thixotropic properties of aqueous dispersions of Laponite RD, *J. Colloid Interface Sci.*, 1996, **182**(2), 501–510.
39 B. Macias-Rodriguez and A. G. Marangoni, Rheological characterization of triglyceride shortenings, *Rheol. Acta*, 2016, **55**(9), 767–779.
40 S. R. Raghavan, Shear-induced microstructural changes in flocculated suspensions of fumed silica, *J. Rheol.*, 1995, **39**(6), 1311.
41 N. A. Burns, *et al.*, Nanodiamond gels in nonpolar media: Colloidal and rheological properties, *J. Rheol.*, 2014, **58**(5), 1599–1614.

